pubs.acs.org/ac

analytical chemistry

June 6, 2025 Volume 97 Number 23

ACS Publications
Most Trusted. Most Cited. Most Read.

www.acs.org

analytical chemistry

pubs.acs.org/ac Article

Modular Centrifugal Microfluidics for Sample Preparation

Ali Gholizadeh,* Gabriel Mazzucchelli, Ana Amoroso, and Tristan Gilet

Cite This: *Anal. Chem.* 2025, 97, 12070−12079 Read Online

ACCESS | Metrics & More | Article Recommendations | Supporting Information

ABSTRACT: Sample preparation is often a critical and labor-intensive step in molecular biology and analytical chemistry. It bottlenecks biological assays, where liquid-handling speed and technique influence the outcome. While automation improves efficiency, traditional systems such as robotic platforms remain costly, complex, and resource-intensive to manufacture. Centrifugal microfluidic devices provide liquid-handling operations at the microliter scale by using microfluidic channels and chambers engraved on disks (Lab-On-A-Disk, LOAD). However, their monolithic design limits flexibility and demands microfluidic expertise, thereby increasing prototyping time and costs, while discouraging broader adoption. To address these limitations, we introduce modular microfluidic chips that are integrable and functional on both LOAD platforms and commercial centrifuges, enabling broad laboratory use without additional equipment. These interchangeable modules perform specific functions—dispensing, metering, mixing, pooling, and collection—without requiring extra components for leak-proof interconnection. Their detachability from the rotating support allows fluid control through "flipping" relative to the centrifugal force. Additionally, they are compatible with multiwell plates and stackable in swinging-bucket centrifuges, enabling high-throughput sample preparation. As a proof of concept, an enzymatic assay was performed by using several assemblies of modules in parallel. After the reagents were mixed and transferred into a well plate, absorbance was measured at three antibiotic concentrations, confirming accurate volume control and reproducible measurements. This modular approach enhances miniaturization, compatibility, and affordability while reducing the reliance on expensive and bulky robotic systems. By simplifying workflows and improving flexibility, this provides an efficient alternative for rapid and scalable sample preparation.

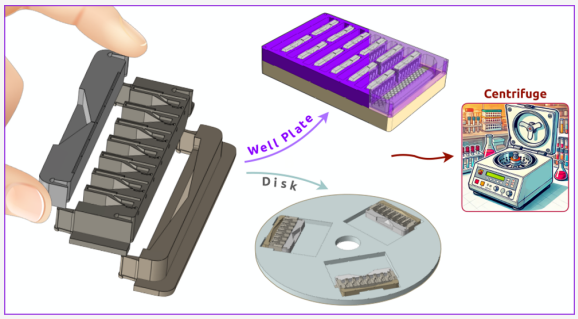

INTRODUCTION

Sample preparation is a critical step in molecular biology and analytical chemistry. It often involves complex workflows, such as those required for cell assays[1] and drug analysis.[2,3] Currently, liquid dispensing/handling is performed either manually by an operator or through specialized robotic equipment. Manual handling, while common, is labor-intensive and prone to variability, introducing a bottleneck in high-throughput applications.[4−6] In contrast, robotic platforms automate sample preparation, reducing human intervention, minimizing errors, and improving the speed and quality of sample preparation.[7] However, these systems are characterized by high upfront costs, technical complexity, and the need for expertise in instrumentation and maintenance. As a result, they are less well-suited for resource-limited environments, such as smaller laboratories, where researchers prioritize affordable and easy-to-use solutions. Centrifugal-assisted techniques have been used in sample preparation for decades.[8] They allow the separation of cells (or even macromolecules in ultra-centrifugation) suspended in a biological sample.[9] Ultra-filtration is also possible by centrifuging tubes containing a low-adsorptive permeable membrane[10] or filter micropipette tips integrated with an appropriate collection tube.[11,12] Such standard platforms may bring user-friendliness, cost-efficiency, and high throughput. However, automation and the combination of multiple centrifuge-based operations remain challenging. Moreover, the selection of appropriate volumes of each sample or reagent still requires intense pipetting, while volume downscaling (miniaturization) is constrained by the pipetting accuracy and quality.

Centrifugal microfluidics enhances miniaturization and automation by seamlessly combining multiple unit operations (e.g., dispensing, metering, mixing, and trapping). With minimal instrumentation, samples can be moved radially outward through microfluidic channels integrated into a rotating platform. Traditionally, this platform is configured as a monolithic microfluidic disk (so-called Lab-On-A-Disk, LOAD).[13] However, the throughput of such systems, namely, the number of assays performed in parallel, is constrained by

Received: January 5, 2025
Revised: May 26, 2025
Accepted: May 27, 2025
Published: June 6, 2025

https://doi.org/10.1021/acs.analchem.5c00076
Anal. Chem. 2025, 97, 12070−12079

Introduction

Sample preparation is a critical step in molecular biology and analytical chemistry. It often involves complex workflows, such as those required for cell assays[1] and drug analysis[2,3]. Currently, liquid dispensing/handling is performed either manually by an operator or through specialized robotic equipment. Manual handling, while common, is labor-intensive and prone to variability, introducing a bottleneck in high-throughput applications[4–6]. In contrast, robotic platforms automate sample preparation, reducing human intervention, minimizing errors, and improving the speed and quality of sample preparation[7]. However, these systems are characterized by high upfront costs, technical complexity, and the need for expertise in instrumentation and maintenance. As a result, they are less well-suited for resource-limited environments, such as smaller laboratories, where researchers prioritize affordable and easy-to-use solutions. Centrifugal-assisted techniques have been used in sample preparation for decades[8]. They allow the separation of cells (or even macromolecules in ultracentrifugation) suspended in a biological sample[9]. Ultrafiltration is also possible by centrifuging tubes containing a low-adsorptive permeable membrane[10] or filter micropipette tips integrated with an appropriate collection tube[11,12]. Such standard platforms may bring user-friendliness, cost-efficiency, and high throughput. However, automation and the combination of multiple centrifuge-based operations remain challenging. Moreover, the selection of appropriate volumes of each sample or reagent still requires intense pipetting, while volume downscaling (miniaturization) is constrained by the pipetting accuracy and quality.

Centrifugal microfluidics enhances miniaturization and automation by seamlessly combining multiple unit operations (e.g., dispensing, metering, mixing, and trapping). With minimal instrumentation, samples can be moved radially outward through microfluidic channels integrated into a rotating platform. Traditionally, this platform is configured as a monolithic microfluidic disk (so-called Lab-On-A-Disk, LOAD)[13]. However, the throughput of such systems, namely the number of assays performed in parallel, is constrained by the dimension of the disk. Furthermore, the monolithic design of the disk introduces a unidirectional application of centrifugal force. Decoupling microfluidic circuits from the disk unlocks some crucial degrees of freedom. It enables flow control in multiple successive directions through the reorientation of the microfluidic circuit with respect to the centrifugal force. On the one hand, systematic reorientation has been achieved by incorporating additional servomotors positioned beneath the chip and mounted on the disk or rotating platform[14–20]. To date, such systems are not widely available, and their development often requires expertise in programming and instrumentation. This may discourage nonexpert users from employing such systems in their applications. On the other hand, manual reorientation of the microfluidic *chip-on-a-disk* systems has been proposed, enabling bidirectional flow control via “flipping” the chip back and forth relative to the direction of centrifugal force[21]. While these systems offered compatibility with traditional LOAD platforms and even standard laboratory equipment such as swinging-bucket centrifuges[22], their functional scope remained limited—typically restricted to isolated tasks like metering or precollection within a single chip—and lacked the flexibility required for more complex or scalable workflows.

In the present study, we overcome these limitations by introducing a modular centrifugal system, in which multiple chips—each corresponding to a distinct module, potentially made from different materials and designed for a specific function—are assembled into a single

device for centrifugation. These modules can be swapped and interconnected, providing flexible and reconfigurable workflows for sample preparation. Such modularity also allows microfluidic units containing embedded elements (e.g., a stirrer blade for mixing[23]) to be separated, cleaned, and reused as standalone modules for several experiments, significantly reducing fabrication time and costs—a key advantage in resource-limited R&D settings. Unlike common modular microfluidic systems that rely on external components such as O-rings[24] or magnets[25] to establish leak-proof connections, our modular design ensures secure liquid transfer solely through geometric interlocking. This offers major benefits, including ease of assembly and integration with well plates, reduced reliance on additional components, and the potential for rapid prototyping. To the best of our knowledge, this modular centrifugal approach is the first to integrate microfluidic modules as a direct replacement for conventional methods to process dozens of samples in parallel while enabling miniaturization.

We first demonstrated a panel of operations with different module assemblies. Then, as a proof of concept, we conducted an enzymatic assay aimed at measuring the concentration of an antibiotic in a sample[26]. The assay involved mixing defined volumes of a sample, an enzyme, and a chromogenic substrate. The antibiotic in the sample immobilized the enzyme and subsequently slowed the substrate conversion to a colored compound. The reaction was halted at a specific time, and the amount of converted substrate was quantified because of an absorbance measurement of the mixture. Eighteen samples at three different (known) concentrations were processed simultaneously through parallel microfluidic circuits.

Experimental Section

Experimental Setup

Each microfluidic system described here comprises an assembly of three main microfluidic modules, designed to perform dispensing, metering/storage/mixing, and collection/pooling. These assemblies were centrifuged in two configurations: chip-*on*-a-disk and chip-*off*-a-disk.

In the chip-*on*-a-disk configuration (Figure 1a), three such assemblies were fixed on a PMMA disk with a vertical rotation axis. The assemblies could be inserted either horizontally, perpendicular to the rotation axis (main schematic of Figure 1a), or vertically in radial planes thanks to a screwed 3D-printed cartridge (inset picture of Figure 1a). The vertical alignment ensured that identical circuits within a module were equidistant from the rotation axis and experienced the same centrifugal force. Modules were positioned a maximum of 5 cm from the rotation axis. A centrifugal bench with a computer-controlled stepper motor rotated the disk at up to 3000 rpm, generating a maximum centrifugal acceleration of 504*g* in the microfluidic chambers with the highest radial position. A high-speed camera Photron AX50 with a macrolens (Zeiss Milvus 2/100M) captured top-view images of the horizontally inserted modules and fluids therein. The motor controller triggered the camera once per rotation, with an exposure time set to 1 µs, achieving an effective resolution of 15 µm.

In the chip-*off*-a-disk configuration (Figure 1b), microfluidic modules were placed in a conventional Eppendorf 5430 centrifuge using 3D-printed supports adapted to a swinging-bucket rotor (A-2-MTP). This centrifuge could be operated at up to 4680 rpm (2204*g* within the bucket). Since the centrifuge was opaque, fluid motion within the modules could not be

imaged in real time. Instead, after centrifugation, the module assemblies were transferred for observation through bright-field microscopy (Zoom Advanced 2, with a camera Canon EOS 5D mark III) with a resolution of 0.5 µm per pixel.

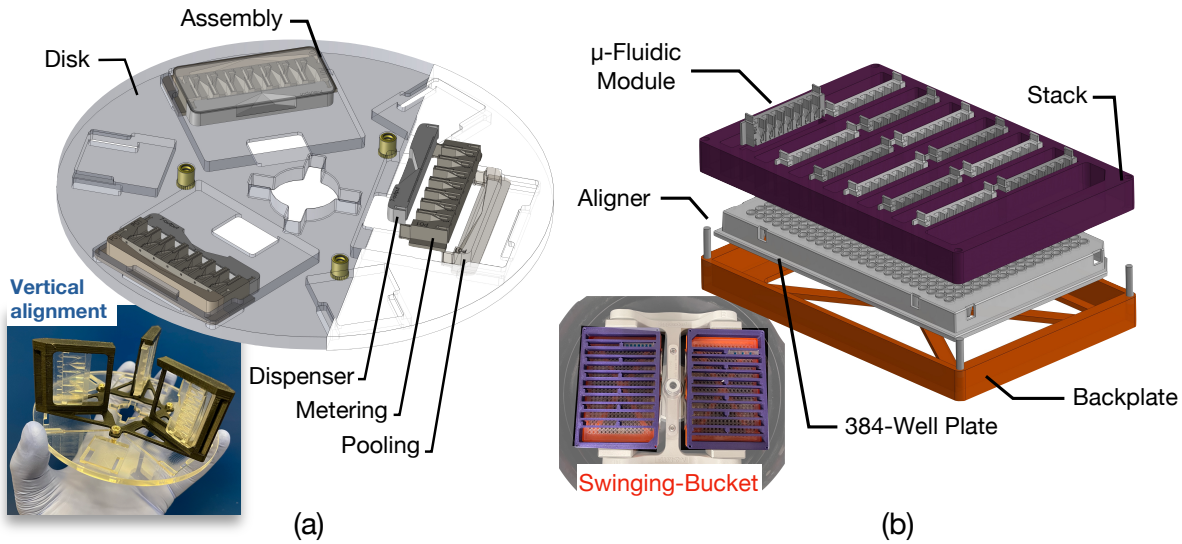

Figure 1: Exploded CAD view of the modular centrifugal microfluidic platform: ***(a)*** *Three assemblies, each with three modules (e.g., dispensing, metering, and pooling), are horizontally inserted into a 12 cm PMMA disk. The inset shows a 3D-printed cartridge (black) screwed to the disk to hold assemblies vertically in radial planes.* ***(b)*** *Module integration with a 384-well plate via a 3D-printed stack and back plate. The inset demonstrates compatibility with a swinging-bucket rotor (A-2-MTP) of the Eppendorf 5430 centrifuge.*

Modules: Design, Fabrication, and Materials

The modular chips used in the experiments were designed with SolidWorks and fabricated by the Sirris Research Center. They were either manufactured in PMMA through a combination of milling and injection molding or 3D-printed in a resin material (Detax Medicalprint, clear-04016). Adhesive tape (Labelor, 3635E5-38B297) was used to cover and seal the microfluidic channels and chambers of each module individually. Five types of rectangular-shaped modules were fabricated with the purpose of dispensing, metering—storing, mixing, collecting, and pooling liquid samples and reagents (Figure 2).

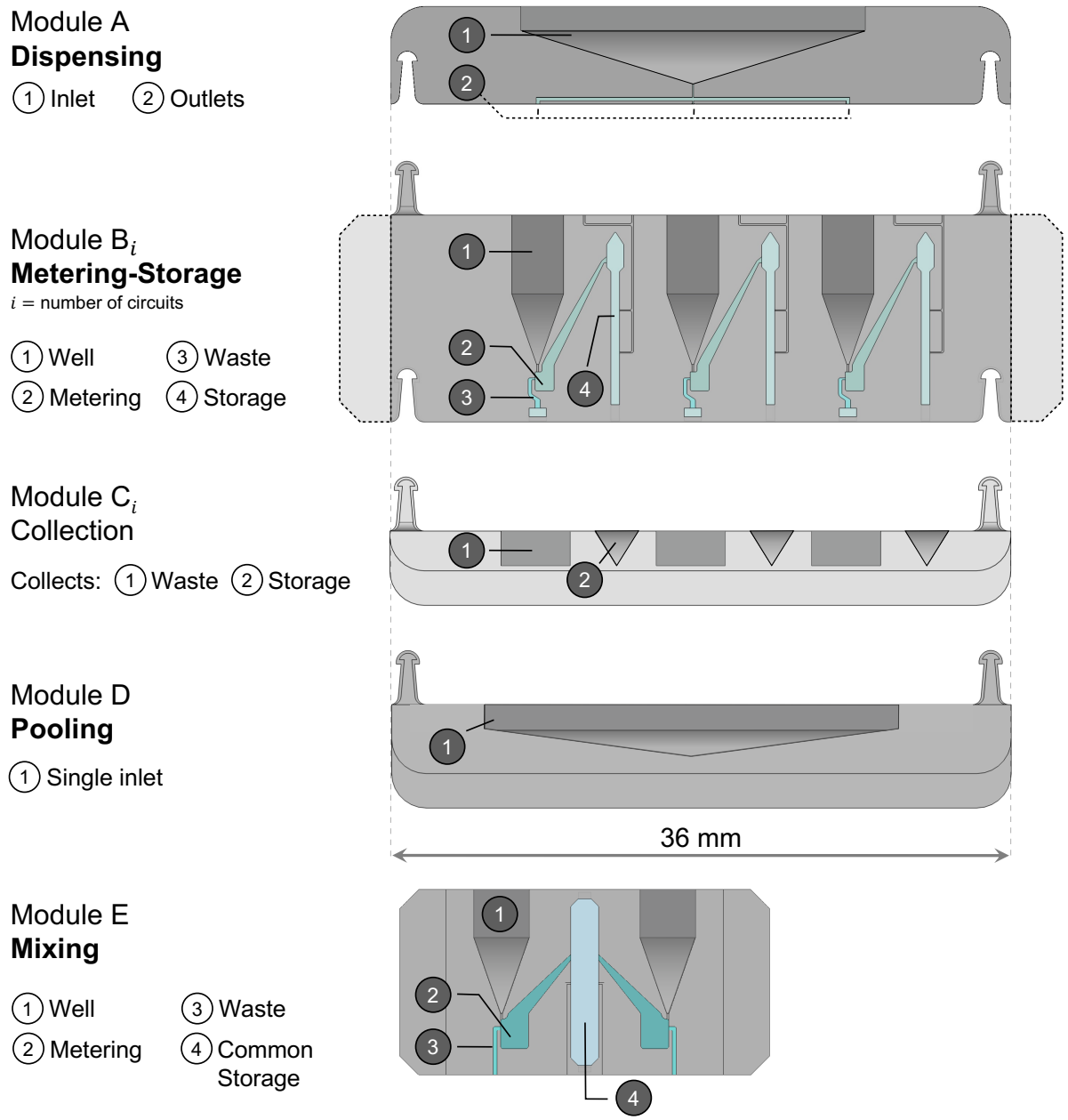

Figure 2: Overview of five types of modules designed for this work: A (dispensing), B_i (metering—storage), C_i (collection), D (pooling), and E (mixing). In B_i and C_i, i indicates the number of identical circuits. Solid colors represent different depths of channels or chambers (values in the main text), while gradients represent tilted surfaces.

Dispensing

The dispensing module (A) was 3D-printed. It was 4 mm thick, 36 mm long, and 7.85 mm wide. It could be assembled into other modules thanks to two female plugs. It comprised a single inlet shaped as a pyramidal well, with a rectangular cross-section of area 60 mm^2 upstream, tapering to 0.006 mm^2 downstream. The module also contained three outlets connected to the well via microfluidic channels: the central channel was 0.1 mm deep, while the two off-centered channels were 0.2 mm deep. The channel leading to the central outlet was designed to be 0.2 mm in length and 0.062 mm in width, whereas the other two channels were 9 mm long and 0.2 mm wide. Consequently, the three channels had approximately the same hydraulic resistance.

Metering and Storage

Three different metering—storage modules were designed and denoted as (B_i), where i = 1, 3, or 7 is the number of identical circuits on the module. Modules (B_3) and (B_7) were 3D-printed in resin, featuring two male and two female assembly plugs. They were 4.9 mm thick and 36 mm long. Module (B_3) was 12 mm wide, and module (B_7) was 9 mm wide. Module (B_1) was PMMA-injected as a block 4.5 mm thick, 20 mm long, and 10 mm wide. The inlet of each circuit was a pyramidal well with a square cross-section of area 9 mm^2 upstream and 0.01 mm^2 downstream. The three wells of (B_3) were spaced by 9 mm (center to center), thereby mirroring the arrangement of the wells in a 96-well plate. The seven wells of (B_7) were spaced by 4.5 mm (center to center), thereby mirroring the arrangement of wells in a 384-well plate. In (B_3) and (B_7), a microfluidic circuit including metering and storage chambers was positioned downstream of each well, while such a circuit was only engraved below the central well of the module (B_1). The outlet of these chambers was designed with a square cross-section of 0.5 $\times$ 0.5 mm^2 to be printed either open or closed. If closed, an injection needle with an external diameter of 600 µm was used for on-demand piercing. In contrast, in (B_1), the outlet was directly machined as open, with a square cross-section of 0.1 $\times$ 0.1 mm^2.

Collection

Two collection modules C_6 and C_7 were designed with six and seven collecting wells, respectively. They were spaced by 4.5 mm, again mimicking the 384-well plates. Each well had a square cross-section of area 9 mm^2 at the inlet. The modules included two male assembly plugs.

Pooling

The pooling module (D) was 3D-printed 4.9 mm thick, 36 mm long, and 4 mm wide. It comprised two male assembly plugs, as well as a single pooling well with a rectangular cross-section of area 100 mm^2 at the inlet.

Mixing

The mixing module (E) was 3D-printed to be 4.5 mm thick, 20 mm long, and 10 mm wide. It comprised two pyramidal wells with a square cross-section of area 9 mm^2 upstream and 0.01 mm^2 downstream. A metering chamber was printed downstream of each well to select a certain volume of the two different samples. Upon simultaneous liquid transfer, these selected volumes could mix in the common storage chamber.

Module Preparation and Testing

Individual modules were rinsed with isopropanol and DI water after fabrication and following each experiment. They were then dried in compressed air and sealed with adhesive tape. Liquid volumes of >10 µL were pipetted into each well of interest. The modules were assembled via geometric interlocking, inspired by the puzzle pieces. Each assembly was then inserted into the support to perform its expected functions upon centrifugation. Modules could be reconfigured before another centrifugation; for example, the metering module could be flipped to transfer the liquid while the other modules retained their orientation.

Application to Enzymatic Assay

As a proof of concept for our modular approach, modules (A), (B_3) and (D) were assembled to conduct an enzymatic assay, on 18 samples simultaneously, in the chip-*off*-a-disk configuration (Figure 1b). Six identical module assemblies were equally positioned between two swinging buckets. Each assembly comprised three identical circuits. Three samples containing different concentrations of piperacillin (0, 25, and 50 µg mL^{-1}, Viatris, India) in 50 mM PBS buffer (KH_2PO_4 1.76 mM, $Na_2HPO_4.2H_2O$ 10 mM, NaCl, 137 mM, KCl 2.7 mM buffer pH 7.4, Sigma-Aldrich, USA) were considered. The blank sample (with no piperacillin) contained only PBS buffer (50 mM). Six circuits from two assemblies were dedicated to each concentration (sixtuplicate). To initiate the assay, 30 µL of nitrocefin (10 mM, Calbiochem, Sigma-Aldrich) was introduced into each module (A). The assemblies were then simultaneously centrifuged at 1000 *g*. Upon centrifugation (step 1), the nitrocefin solution was distributed into each well of the modules (B_3), and metering of 2 µL per circuit was subsequently achieved in less than 30 seconds (the minimum centrifugation time of our Eppendorf centrifuge). Excess liquid was effectively directed to the pooling module (D) via the dedicated waste channel. Then, each pooling module was removed, and the remaining assemblies were repositioned upside-down in the swinging buckets. Upon centrifugation at 1000*g* for 30 s (step 2), three metered nitrocefin solutions in module (B_3) were transferred into their respective storage chambers. This process (steps 1 and 2) was similarly repeated to transfer an additional and identical volume of nitrocefin into the storage chamber, then 2 µL of piperacillin and finally 2 µL of enzyme P99 (0.036 U/µL). After stopping the centrifugation, the enzymatic reaction was allowed to proceed for precisely 2 min. During this interval, all storage chambers were manually pierced to open their outlets, enabling the transfer of the mixed solutions into two 96-well plates, each aligned beneath the assemblies per swinging bucket. The accurate alignment of the storage chamber outlets with the wells was achieved through carefully designed 3D-printed supports. The wells were initially loaded with 92 µL of acetate buffer. Finally, centrifugation was resumed at 2204*g* for 60 s, simultaneously transferring and collecting the mixture from each circuit into the well plates. The preloaded buffer immediately halted the enzymatic reaction. The resulting absorbance at 480 nm was measured in each well by using a UV—vis spectrophotometer (Tecan Infinite F50 Robotic, accuracy within 3%). Three other experiments were conducted, each using one assembly of the same module type, to verify the reproducibility of the results.

Results

Dispensing

The time sequence of the dispensing process is illustrated in Figure 3. It involved an assembly of modules (A), (B_3) and (C_6). The waste outlets of the module (B_3) were initially closed (i.e., not pierced yet). A volume of 52 µL of blue-dyed water was loaded in the single well of the dispensing module (A). The latter was assembled to modules (B_3) and (C_6), then centrifuged at an initial speed of 1700 rpm (~100*g* at r ≅ 3 cm for the dispensing module) (t = 1.65 s). At that speed, the liquid remained blocked at the outlets of the module (A) (annotated as capillary valve in Figure 3), since the corresponding centrifugal acceleration was below the threshold (~125*g* corresponding to a 3 mm liquid column from the well inlet to the outlet at t

= 1.65 s) to overcome the capillary pressure associated with the sudden increase of the channel cross-section. As the rotational speed was increased to 2000 rpm (~134*g* at r ≅ 3 cm for the dispensing module), the liquid started to drip from the three outlets, into the facing inlet wells of the module (B_3). The liquid accumulated within the circuits of this module. However, since the waste outlets of (B_3) were closed (*t* = 2.73 s), any liquid transfer to the module (C_6) was prevented. Consequently, the liquid remained in a quasi-hydrostatic state, with the liquid level gradually increasing in all three circuits (*t* = 5.73 s). Ultimately, the inlet volume was split into three subvolumes (~17 µL), demonstrating that the 3D-printed microchannels provided similar hydraulic resistance (*t* = 7.53 s). Any remaining liquid in (A) could be flushed toward (B_3) by increasing the rotational speed.

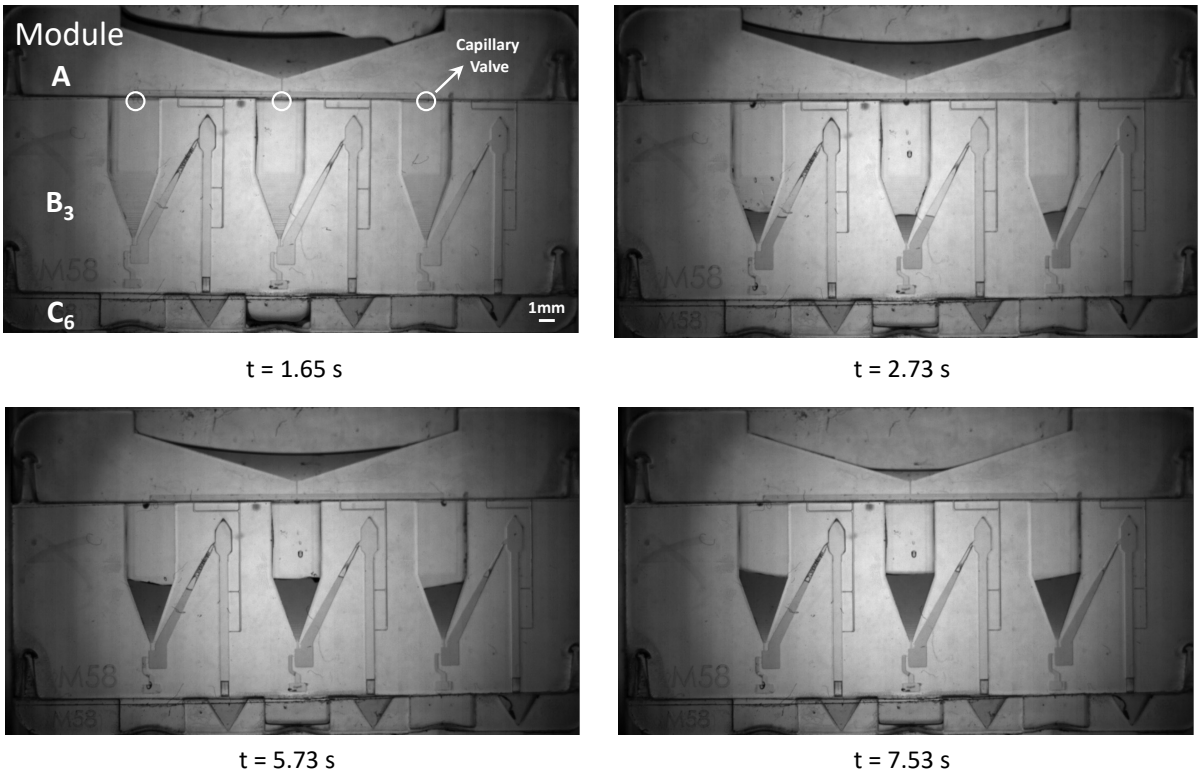

Figure 3: Snapshots of dyed water dispensing from module (A) to module (B_3), assembled with module (C_6). At 1700 rpm (t = 1.65 s), the waste outlets of (B_3) remained closed, preventing capillary valve bursting. The rotational speed was then increased to 2000 rpm for even distribution across microfluidic circuits. Snapshots (from t = 2.73 to t = 7.53 s) show dispensing and distribution into (B_3) wells at 2000 rpm. During this process, liquid volumes remained in a quasi-hydrostatic state within (B_3) ***(See Supporting Information Video S1).***

Metering and Collection

Once liquid distribution was completed, the modules were disassembled to pierce the waste outlets of the module (B_3). The modules were assembled again. They were then centrifuged with an rotational speed ramping from 100 to 2000 rpm in 1.90 s. Figure 4a (top) represents snapshots taken during the metering process. Upon centrifugation, the accumulated liquid within each circuit was gated to the waste channel of (B_3) and transferred to the module (C_6), except for the liquid trapped in the metering chambers. Metering was completed in less than 5 s. The three chambers selected different liquid volumes: 76 nL (left), 101 nL (middle), and 139 nL (right), corresponding to a coefficient of variation (CV) across chambers of 28%. This variation was caused by uneven alignment with centrifugal force. This effect was mitigated

when the assemblies of modules were centrifuged in a vertical position (inset of Figure 1a). Figure 4a (bottom) illustrates an even volume selection, with a CV across chambers of less than 3%. To assess reproducibility, experiments were repeated twice for each orientation of module (B3), and the corresponding volumes are presented in Figure 4b. In either configuration, the volume selection was found to be systematic and reproducible with a CV of less than 5% for each chamber across the three experiments.

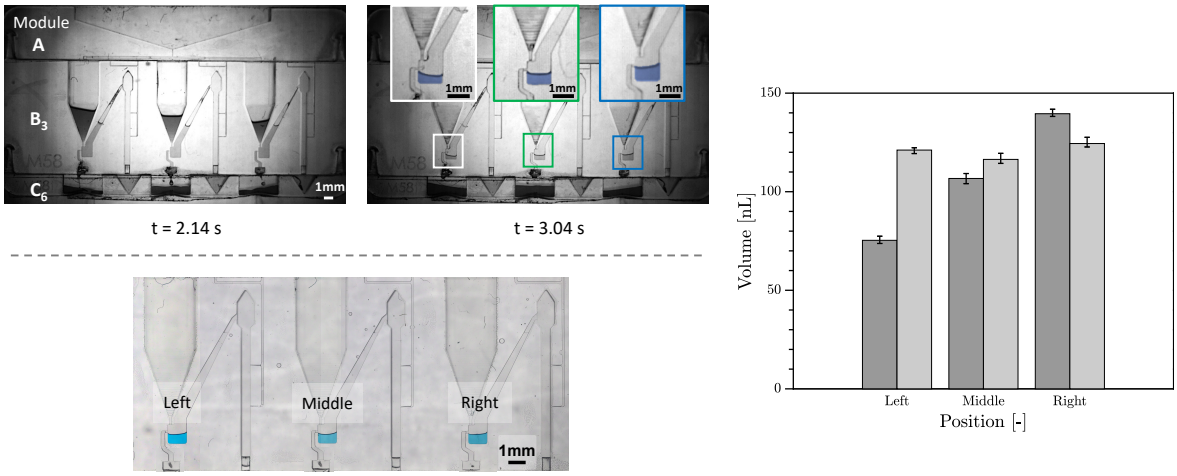

a) b)

Figure 4: Metering step with an assembly of modules (A), (B_3), and (C_6) positioned on the disk in two orientations: (a, top) horizontal and (a, bottom) vertical. In both cases, the waste outlets of (B_3) were pierced. ***(a, top)*** *During centrifugation at 2000 rpm, excess liquid was gated and collected in (C_6) (t = 2.14 s). A given volume was selected in each metering chamber with a nominal volume of 143 nL within one second (t = 3.04 s). Insets show a close-up of the three metering chambers, where the trapped volume appears in blue.* ***(a, bottom)*** *Even selection of blue dye liquid was achieved within three metering chambers after centrifugation at 2000 rpm.* ***(b)*** *Bar chart comparing the measured volume trapped within the metering chambers at different positions (left, middle, and right). Dark and light gray bars represent volume variations when the module B_3 is oriented horizontally and vertically on the disk, respectively, highlighting improved volume uniformity in the vertical configuration.*

Scaling Up the Throughput by Stacking the Modules

The throughput of the system can be significantly increased by stacking multiple modules (e.g., modules B_3 and/or B_7). In this arrangement, the waste outlets of one module are precisely aligned with the inlets of the next. The temporal progression of such a combined metering process is demonstrated in Figure 5 for three assembled modules. Modules 1 and 2 correspond to the (B_7) design, and they were 3D-printed. Module 3 corresponds to the (B_1) design. The wells therein were made by injection molding, while the microfluidic circuits were machined. First, 10 µL of blue-dyed water was pipetted into each of the three wells of module 1. The assembly was centrifugated, again with a ramp from 100 to 2000 rpm within 1.90 s. The capillary valves at the well outlets of module 1 burst once the rotational speed reached 850 rpm (t = 0.75 s), allowing the liquid to initially fill the metering chambers of module 1. The liquid in excess was subsequently directed to the waste channels of module 1. It then dripped into the wells of module 2 (t = 0.88 s). Again, after the metering chambers of module 2 were filled, the water in excess was channeled to the wells of module 3 (t = 1.10 s). Volume selection was achieved in all the metering chambers in less than 2.50 s. The liquid still in excess was accumulated in the wells of module 3, where it could potentially be recycled, e.g., by being transferred to other modules, or even to conventional well plates (Figure S1 in Supporting Information).

Successive Centrifugations

In sample preparation, successive steps may be necessary to add different reagents, downscale their volumes, accumulate them in storage chambers, and finally retrieve them in the collection module or in a conventional well plate. Figure 6 demonstrates a comprehensive fluidic workflow achieved by combining different microfluidic functions. Blue-dyed water with a volume of 10 µL was introduced into the metering-storage module (B_3), for which both the waste and the storage outlets were initially closed. Upon centrifugation at 2000 rpm (224*g*), the liquid accumulated in the well and the circuit downstream (Figure 6a). If denser particles or cells were present, this step would cause their sedimentation at the bottom of the metering chamber (Figure S2 in the Supporting Information). Then the waste outlet was pierced (Figure 6b) and a second centrifugation led to the selection of approximately 100 nL in the metering chamber (Figure 6c). This volume was then transferred to the storage chamber upon flipping and centrifugation. This process was repeated 8 times, resulting in a total volume of approximately 800 nL in the storage chamber (Figure 6d). Finally, the storage outlet was pierced, the module (B_3) was assembled to a collection module (C_6), and the liquid was transferred from the storage chamber to the collection well upon centrifugation at 3000 rpm (504*g*) (Figure 6e).

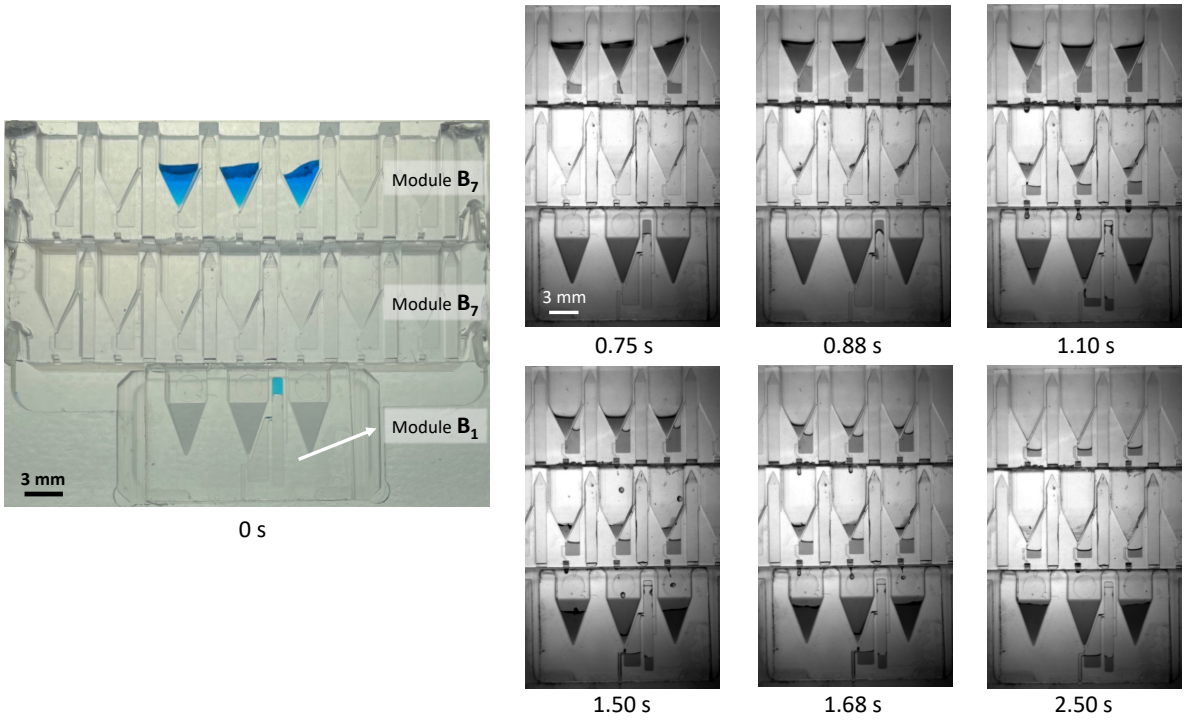

Figure 5: Time sequence of centrifuging three microfluidic modules (two B_7 and one B_1): At t = 0 s, 10 µL of dyed water was added to each well of the first (B_7) module. The assembly was spun from 100 to 2000 rpm over 1.90 s. Liquid entered the microfluidic circuits of the first (B_7) module at 850 rpm (t = 0.75 s) and began dripping into the wells of the second (B_7) module at t = 0.88 s. Similar metering occurred in the second (B_7) module, with excess liquid transferring to the wells of module (B_1). At 1200 rpm (t = 1.10 s), liquid in (B_1)'s storage chamber moved to its bottom. Metering in all modules completed by t = 2.50 s ***(See Supporting Information Video S2).***

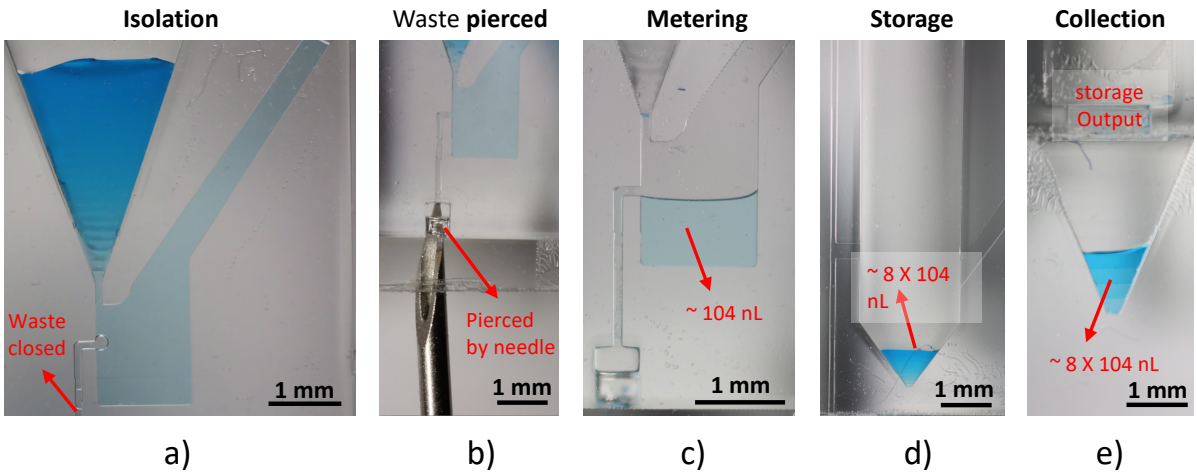

Figure 6: Sequence of microfluidic functions using modules (B_3) and (C_6). Initially, waste and storage outlets were printed closed. ***(a)*** *After adding 10 µL of blue-dyed water to a (B_3) well, centrifugation at 2000 rpm (224g) filled the microfluidic circuit.* ***(b)*** *The waste outlet was pierced with a needle.* ***(c)*** *Centrifugation at 2000 rpm metered ~100 nL in less than 10 s.* ***(d)*** *This volume was transferred to the storage chamber via flipping and centrifugation, repeated 8 times to store ~800 nL.* ***(e)*** *Finally, the storage outlet was pierced, and the liquid transferred to module (C_6) via centrifugation at 3000 rpm (504g).*

Mixing Blue and Red Dyes

The mixing functionality of the modular centrifugal microfluidic platform was demonstrated using module (E). Initially, 10 µL of blue-dyed and red-dyed water were pipetted into the left and right wells of module (E), respectively (Figure 7a). Upon centrifugation at 504*g*, 700 nL of each solution was selected in the respective metering chambers within 10 s (Figure 7b), while the excess liquid was directed to a pooling module (D) integrated beneath module (E). Subsequently, module (E) was detached from module (D), flipped to reorient the liquid-filled metering chambers, and centrifuged again at 504*g*. Upon centrifugation, the dyes were dislodged from the metering chambers and mixed in the common storage chamber of module (E) (Figure 7c). A marginal volume of each solution remained in the metering chambers.

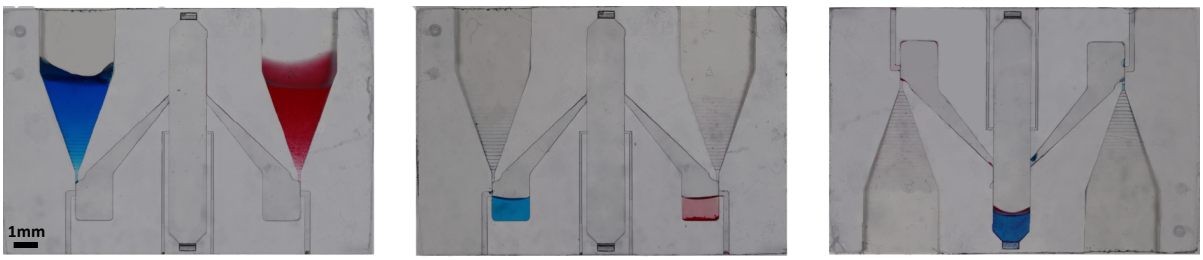

Figure 7: Mixing blue- and red-dyed water samples using module (E): ***(a)*** *10 µL of each solution was added to the left and right wells of module (E), respectively.* ***(b)*** *Centrifugation at 504 g for 10 s selected 700 nL of each sample into the associated metering chambers, with excess liquid directed to pooling module (D) but not visible here.* ***(c)*** *Module (E) was detached from (D), flipped, and centrifuged again at 504 g to transfer the solutions to the storage chamber for mixing.*

Enzymatic Assay

An enzymatic assay was conducted to demonstrate the applicability of our modular centrifugal system. A single experiment yielded 18 simultaneous absorbance measurements, corresponding to six replicates each at piperacillin concentrations of 0 (blank), 25, and 50 µg

mL^{-1} (Figure 8). The CV for the absorbance values was calculated to be less than 10% for all concentrations. It proves that reagents were accurately and reproducibly metered and transferred through this multiple-step workflow.

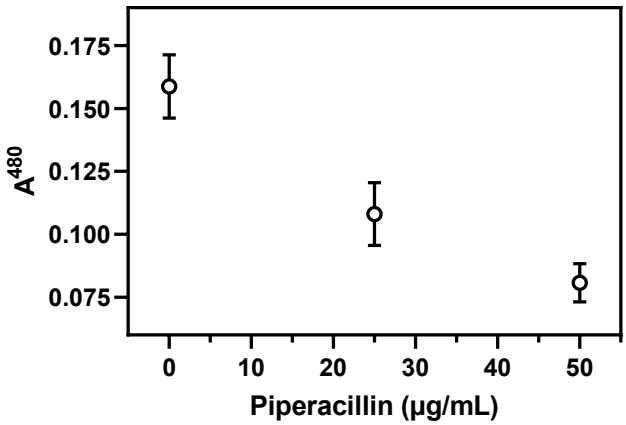

Figure 8: Piperacillin concentrations (0, 25, and 50 µg mL^{-1}) measured via reporter substrate absorbance at 480 nm. The error bars correspond to mean ± standard deviation. The corresponding CV was less than 10%.

Discussion

The microfluidic modules and centrifugation systems proposed in this work mirror LOAD platforms[27] while offering enhanced flexibility and portability. Modules with different materials and microfluidic designs can be assembled on the same disk.

When liquids are manually pipetted, microbubbles may form within the inlet well of the associated module. Thanks to centrifugation, these bubbles rise to the liquid—gas interface, eventually pop, and disappear. Bubbles with sizes comparable to those of the microfluidic features may become trapped at low centrifugation speeds. Nevertheless, the maximum size of such bubbles is bounded by the effective capillary length[21]. This length can be made smaller than the microfluidic features by increasing the centrifugal acceleration, thereby preventing bubble trapping.

Following centrifugation, liquids are efficiently transferred between interconnected modules without any visible leak. If there were any leakage, it would happen during centrifugation—within the enclosed centrifuge—thus minimizing any risk to users or the laboratory environment. The inlet of downstream modules is deliberately designed ten times larger than the outlet of upstream modules to effectively capture any liquid drop or jet that would be deviated by Coriolis[28] and/or Euler[29] forces (e.g., Figure 3 illustrates the accumulation of the dispensed volume in the well of the module downstream of the dispensing module). This feature eliminates the need for external sealing components[30] such as O-rings, reducing manufacturing costs and simplifying assembly while maintaining reliable liquid transfer during operation. This is well-suited for applications where dead volume within tubing connections needs to be minimized[31].

Dispensing modules (A) would have to be fabricated with exceptional precision if they were expected to ensure an even distribution of the inlet volumes into downstream wells. The strategy implemented in this work consisted of adjoining a metering module downstream of the dispensing module. This metering module could largely compensate any uneven

distribution by the dispensing module and select reproducible volumes in each chamber (Figure 3 and 4). The use of dispensing modules in combination with metering modules, as introduced in this work, may provide a potential alternative to manual pipetting for sample preparation, significantly reducing the number of pipetting steps while enabling miniaturization at the submicroliter scale.

Unlike most LOAD systems, where microfluidic features are designed in cylindrical coordinates[32], the microfluidic modules in this work were designed in Cartesian coordinates, which is faster and simpler. However, in the in-plane chip-*on*-a-disk configuration, identical chambers in different circuits are positioned at varying effective distances from the rotation axis and orientations, leading to uneven centrifugal forces and potential variations in the metered volume (Figure 4a, top). While the middle chamber is perfectly aligned with the centrifugal acceleration, the additional force components affected the left and right chambers differently. Specifically, the centrifugal force pushed the selected volume toward the waste outlet in the left chamber and against the vertical wall in the right chamber, resulting in the smallest (76 nL) and largest (139 nL) metered volumes, respectively. Although significant, this variation was systematic and reproducible, with CVs below 5% across repeated experiments for each chamber (Figure 4b). This issue was resolved in the "vertical alignment" configuration of Figure 1a, where all circuits within each module were placed in radial planes and equidistant from the rotation axis. Therefore, consistent metered volumes were obtained (Figure 4a-bottom), with an average CV below 5%, across chambers and experimental replicas (Figure 4b). In the swinging buckets (Figure 1b), the assemblies are positioned such that the centrifugal force has its main component in the downstream direction, and a secondary component in the direction normal to the microfluidic plane. The contribution of the primary component decreases as the assemblies are placed farther from the radial plane passing through the bucket center. This results in slower flows, but it does not prevent proper metering and liquid transfer in any of the modules. The secondary component, being normal to the plane of the microfluidic features, does not generate any significant flow. Therefore, the module positioning in the swinging bucket ensures consistent unit operation across all the circuits, with a distribution of centrifugal force that is similar to that of the vertical alignment on the disk.

Figure 6 demonstrates the system functionality, particularly for centrifuge-based sample preparation. The process involves sequential liquid addition, volume reduction, accumulation in storage chambers, and final retrieval in the collection module. For biological samples, including cells, the metering—storage module outlet (B_3) can be temporarily closed to enable cell isolation and trapping within the metering chamber. In this quasi-hydrostatic state, denser cells sediment at their terminal velocity, where centrifugal force and Stokes drag[33] are balanced (Figure S2). Herein, we demonstrated that the modules performed reliably when fabricated either in PMMA, in COC, or with a commercial 3D-printing resin—all of which are biocompatible materials. They are likely to perform well when made from other biocompatible polymers such as PC, PS or PP. By combining biocompatibility and miniaturization, this modular approach is well-suited for low-cell assays. Cells can be manually pipetted in the inlet wells of the modules or automatically deposited via Fluorescence-Activated Cell Sorting (FACS) for high-throughput analysis[1].

The mixing functionality of the modular centrifugal microfluidic platform was demonstrated using module (E), which combined metering and mixing to blend defined submicroliter volumes of dyed water. Mixing was achieved by flipping the module back and forth relative to the centrifugal force, a step that can be repeated for applications seeking a higher homogeneity. This novel centrifuge-based mixer relies on a passive mechanism[34–36], leveraging chaotic advection flows without external components (e.g., stirrer blade[23]). It is particularly advantageous for applications involving delicate species or molecules, such as cells or proteins, where low shear mixing minimizes the risk of damage, preserving the integrity of the samples. Optimization could enhance the interpenetration between the two fluids.

A proof of concept was demonstrated via absorbance measurements, validating system functionality with an enzymatic assay. Multiple reactions were performed, quantifying nitrocefin hydrolysis in the presence of piperacillin. To assess reproducibility, three experiments were conducted, each using a single assembly. However, variations in reaction stopping time could introduce errors. In contrast, centrifuging six assemblies simultaneously increased throughput while maintaining reasonable accuracy (CV < 10%, Figure 8), with metering accuracy as the primary error source (CV < 7%). Further optimization of the metering module design and improving 3D printing quality could enhance precision. This proof of concept highlights the advantages of our modular approach, demonstrating its flexibility and compatibility with commercial centrifuges and well plates. It also confirmed that repeated assembly and disassembly of the modules did not adversely affect the reproducibility or precision of the results. Throughput can be significantly increased by expanding the well plate capacity and stacking modules, thereby enabling scalable parallel assays and multiplexed applications, as well as reducing waste (Figure 5). This approach also shows the potential for high-throughput biomolecule detection. With adaptations, it may support a wide range of the biological applications previously explored using centrifugal microfluidics. This includes solid-phase extraction[20] for sample preparation, e.g., for Therapeutic Drug Monitoring (TDM)[37] as long as full automation is not strictly required.

Conclusions

This study presented a novel modular centrifugal microfluidic platform designed for sample preparation that addresses key limitations of traditional LOAD systems, such as their monolithic design and reliance on dedicated centrifugation setups. It features interchangeable modules, each performing a distinct function—dispensing, metering, mixing, pooling, and collection—that can be combined to streamline and accelerate sample preparation processes. As these modules are temporarily assembled through geometric interlocking, they can be individually reoriented at any time to gain full control of liquid transfer in the microfluidic circuits. They can be flexibly positioned and removed from a variety of rotating supports, including commercial swinging-bucket centrifuges. The platform also supports scalability by enabling the stacking of similar modules in the radial direction for high-throughput parallel processing. A proof-of-concept enzymatic assay was demonstrated with simultaneous operation in multiple modules, where absorbance was measured at different antibiotic concentrations. Measurements were obtained at once by performing a sequence of elementary operations (dispensing, metering, mixing, etc.) on many samples in parallel.

In conclusion, our approach enables a semiautomated workflow: it significantly reduces human intervention compared to conventional pipetting-based protocols, but it does not achieve full automation offered by robotic systems. This modular centrifugal microfluidic system provides a robust and cost-effective solution for sample preparation workflows, combining miniaturization to reduce reagent use, scalability for high-throughput applications, and partial automation to enhance efficiency and reproducibility. Additionally, its ease of use and compatibility with standard multiwell plates and swinging bucket centrifuges make it suitable for a wide range of applications, including experimental design and development tests, sample preparation for next-generation sequencing, PCR, ELISA, TDM, one-pot proteomic workflows, and even single-cell proteomics. Future developments will focus on improving precision and expanding application areas, paving the way for broader adoption in research and clinical laboratories worldwide.

Associated content

Supporting information

The Supporting Information is available free of charge at https://pubs.acs.org/doi/10.1021/acs.analchem.5c00076.

- Experimental details on liquid transfer and cell trapping (PDF)
- Dyed water dispensing from module (A) to module (B3), assembled with module (C6) (MOV)
- Centrifuging dyed water through the assembly of three microfluidic modules (two B7 and one B1) (MP4)

Acknowledgements

The authors thank the FAB52 workshop at the A&M department for their support with FDM 3D printing, Denis Vandormael (Sirris) for manufacturing the microfluidic chips, and Bernard Joris for his insightful discussions on the application of this work. This research was funded by the Wallonia Public Service (SPW) through the Win2Wal grant 2010126 (ChipOmics).

Author contributions

Ali Gholizadeh: Conceptualization, Methodology, Software, Experiments, Data processing, Validation, Formal Analysis, Investigation, Writing – Original Draft, Writing – Critical Review & Editing, Visualization.
Gabriel Mazzucchelli: Conceptualization, Writing – Critical Review & Editing (Commentary or Revision), Project Administration.
Ana Amoroso: Experiment (application), Validation, Formal Analysis, Writing – Review & editing.
Tristan Gilet: Conceptualization, Validation, Resources, Writing – Critical Review & Editing (Commentary or Revision), Supervision.

Table of content (TOC)

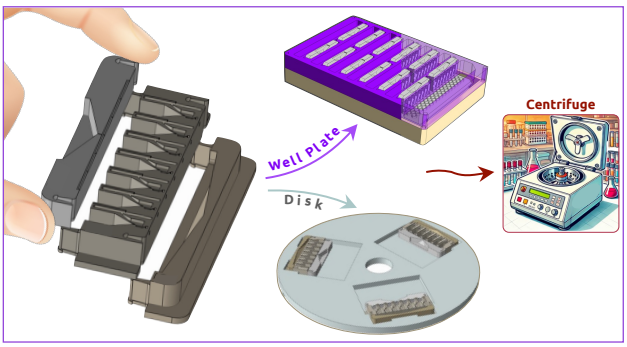

References

(1) Kassem, S.; Van Der Pan, K.; De Jager, A. L.; Naber, B. A. E.; De Laat, I. F.; Louis, A.; Van Dongen, J. J. M.; Teodosio, C.; Díez, P. Proteomics for Low Cell Numbers: How to Optimize the Sample Preparation Workflow for Mass Spectrometry Analysis. *J Proteome Res* **2021**, *20* (9), 4217–4230. https://doi.org/10.1021/ACS.JPROTEOME.1C00321/ASSET/IMAGES/LARGE/PR1C00321_0002.JPEG.

(2) Fu, X.; Liao, Y.; Liu, H. Sample Preparation for Pharmaceutical Analysis. *Anal Bioanal Chem* **2005**, *381* (1), 75–77. https://doi.org/10.1007/s00216-004-2894-5.

(3) Namera, A.; Saito, T. Advances in Monolithic Materials for Sample Preparation in Drug and Pharmaceutical Analysis. *TrAC - Trends in Analytical Chemistry*. Elsevier B.V. 2013, pp 182–196. https://doi.org/10.1016/j.trac.2012.10.017.

(4) Xia, L.; Yang, J.; Su, R.; Zhou, W.; Zhang, Y.; Zhong, Y.; Huang, S.; Chen, Y.; Li, G. Recent Progress in Fast Sample Preparation Techniques. *Analytical Chemistry*. American Chemical Society January 7, 2020, pp 34–48. https://doi.org/10.1021/acs.analchem.9b04735.

(5) Niu, Z.; Zhang, W.; Yu, C.; Zhang, J.; Wen, Y. Recent Advances in Biological Sample Preparation Methods Coupled with Chromatography, Spectrometry and Electrochemistry Analysis Techniques. *TrAC - Trends in Analytical Chemistry*. Elsevier B.V. May 1, 2018, pp 123–146. https://doi.org/10.1016/j.trac.2018.02.005.

(6) Dehghan, A.; Kiani, M. J.; Gholizadeh, A.; Aminizadeh, J.; Rahi, A.; Zare, I.; Pishbin, E.; Heli, H. Electrochemical Genosensors On-a-Chip: Applications in Early Diagnosis of Pathogens. *Sensors and Actuators Reports* **2025**, *9*, 100335. https://doi.org/10.1016/J.SNR.2025.100335.

(7) More, D.; Khan, N.; Tekade, R. K.; Sengupta, P. An Update on Current Trend in Sample Preparation Automation in Bioanalysis: Strategies, Challenges and Future Direction. *Critical Reviews in Analytical Chemistry*. Taylor and Francis Ltd. 2024. https://doi.org/10.1080/10408347.2024.2362707.

(8) Suwanvecho, C.; Krčmová, L. K.; Švec, F. Centrifugal-Assisted Sample Preparation Techniques: Innovations and Applications in Bioanalysis. *TrAC - Trends in Analytical Chemistry*. Elsevier B.V. November 1, 2024. https://doi.org/10.1016/j.trac.2024.117909.

(9) Völkl, A. Ultracentrifugation. *Encyclopedia of Life Sciences* **2010**. https://doi.org/10.1002/9780470015902.A0002969.PUB2.

(10) Toma, C. M.; Imre, S.; Vari, C. E.; Muntean, D. L.; Tero-Vescan, A. Ultrafiltration Method for Plasma Protein Binding Studies and Its Limitations. *Processes 2021, Vol. 9, Page 382* **2021**, *9* (2), 382. https://doi.org/10.3390/PR9020382.

(11) Song, Y.; An, Y.; Liu, W.; Hou, W.; Li, X.; Lin, B.; Zhu, Z.; Ge, S.; Yang, H. H.; Yang, C. Centrifugal Micropipette-Tip with Pressure Signal Readout for Portable Quantitative Detection of Myoglobin. *Chemical Communications* **2017**, *53* (86), 11774–11777. https://doi.org/10.1039/C7CC07231G.

(12) Qian, C.; Li, J.; Pang, Z.; Xie, H.; Wan, C.; Li, S.; Wang, X.; Xiao, Y.; Feng, X.; Li, Y.; Chen, P.; Liu, B. F. Hand-Powered Centrifugal Micropipette-Tip with Distance-Based Quantification for on-Site Testing of SARS-CoV-2 Virus. *Talanta* **2023**, *258*, 124466. https://doi.org/10.1016/J.TALANTA.2023.124466.

(13) Madou, M.; Zoval, J.; Jia, G.; Kido, H.; Kim, J.; Kim, N. Lab on a CD. *Annual Review of Biomedical Engineering*. 2006, pp 601–628. https://doi.org/10.1146/annurev.bioeng.8.061505.095758.
(14) Xiaobao Cao; J. deMello, A.; S. Elvira, K. Enhanced Versatility of Fluid Control in Centrifugal Microfluidic Platforms Using Two Degrees of Freedom. *Lab Chip* **2016**, *16* (7), 1197–1205. https://doi.org/10.1039/C5LC01530H.
(15) Miao, B.; Peng, N.; Li, L.; Li, Z.; Hu, F.; Zhang, Z.; Wang, C. Centrifugal Microfluidic System for Nucleic Acid Amplification and Detection. *Sensors 2015, Vol. 15, Pages 27954-27968* **2015**, *15* (11), 27954–27968. https://doi.org/10.3390/S151127954.
(16) Geissler, M.; Clime, L.; Hoa, X.; … K. M.-A.; 2015, undefined. Microfluidic Integration of a Cloth-Based Hybridization Array System (CHAS) for Rapid, Colorimetric Detection of Enterohemorrhagic Escherichia Coli (EHEC) Using. *ACS PublicationsM Geissler, L Clime, XD Hoa, KJ Morton, H Hébert, L Poncelet, M Mounier, M DeschênesAnalytical chemistry, 2015•ACS Publications*.
(17) Li, L.; Miao, B.; Li, Z.; Sun, Z.; Peng, N. Sample-to-Answer Hepatitis B Virus DNA Detection from Whole Blood on a Centrifugal Microfluidic Platform with Double Rotation Axes. *ACS Sens* **2019**, *4* (10), 2738–2745. https://doi.org/10.1021/ACSSENSORS.9B01270.
(18) Chen, Y.; Zhu, Y.; Shen, M.; Lu, Y.; Cheng, J.; Xu, Y. Rapid and Automated Detection of Six Contaminants in Milk Using a Centrifugal Microfluidic Platform with Two Rotation Axes. *Anal Chem* **2019**, *91* (12), 7958–7964. https://doi.org/10.1021/ACS.ANALCHEM.9B01998.
(19) Zhu, Y.; Chen, Y.; Meng, X.; Wang, J.; Lu, Y.; Xu, Y.; Cheng, J. Comprehensive Study of the Flow Control Strategy in a Wirelessly Charged Centrifugal Microfluidic Platform with Two Rotation Axes. *Anal Chem* **2017**, *89* (17), 9315–9321. https://doi.org/10.1021/ACS.ANALCHEM.7B02080.
(20) Carthy, É.; Hughes, B.; Higgins, E.; Early, P.; Merne, C.; Walsh, D.; Parle-McDermott, A.; Kinahan, D. J. Automated Solid Phase DNA Extraction on a Lab-on-a-Disc with Two-Degrees of Freedom Instrumentation. *Anal Chim Acta* **2023**, *1280*, 341859. https://doi.org/10.1016/J.ACA.2023.341859.
(21) Gholizadeh, A.; Mazzucchelli, G.; Gilet, T. Flipping: A Valve-Free Strategy to Control Fluid Flow in Centrifugal Microfluidic Systems. *Sens Actuators B Chem* **2024**, *412*. https://doi.org/10.1016/j.snb.2024.135778.
(22) Gholizadeh, A.; Mazzucchelli, G.; Kune, C.; Gilet, T. Fluidic Unit for Discrete Element Trapping. WO2024175769A1, 2024. https://hdl.handle.net/2268/321611.
(23) Dehghan, A.; Gholizadeh, A.; Navidbakhsh, M.; Sadeghi, H.; Pishbin, E. Integrated Microfluidic System for Efficient DNA Extraction Using On-Disk Magnetic Stirrer Micromixer. *Sens Actuators B Chem* **2022**, *351*. https://doi.org/10.1016/j.snb.2021.130919.
(24) Lee, K. G.; Park, K. J.; Seok, S.; Shin, S.; Kim, D. H.; Park, J. Y.; Heo, Y. S.; Lee, S. J.; Lee, T. J. 3D Printed Modules for Integrated Microfluidic Devices. *RSC Adv* **2014**, *4* (62), 32876–32880. https://doi.org/10.1039/c4ra05072j.
(25) Ecker, R.; Langwiesner, M.; Mitteramskogler, T.; Fuchsluger, A.; Hintermuller, M. A.; Jakoby, B. Modular Microfluidic PDMS Blocks Using a Magnetic Connection System. In *Proceedings of IEEE Sensors*; Institute of Electrical and Electronics Engineers Inc., 2022; Vol. 2022-October. https://doi.org/10.1109/SENSORS52175.2022.9967037.

(26) Brans, A.; Joris, B.; Delmarcelle, M.; Jacueline, M.; Tulkens, P.; Hammaecher, C.; Goormaghtigh, E.; De Coninck, J. Method for Measuring Beta-Lactam Antibiotics. WO2013053953A1, 2013.
(27) Ducrée, J.; Haeberle, S.; Lutz, S.; Pausch, S.; Von Stetten, F.; Zengerle, R. The Centrifugal Microfluidic Bio-Disk Platform. *Journal of Micromechanics and Microengineering* **2007**, *17* (7). https://doi.org/10.1088/0960-1317/17/7/S07.
(28) En Lin, S. I. A Novel Splitter Design for Microfluidic Biochips Using Centrifugal Driving Forces. *Microfluid Nanofluidics* **2010**, *9* (2–3), 523–532. https://doi.org/10.1007/S10404-010-0568-5/FIGURES/14.
(29) Deng, Y.; Fan, J.; Zhou, S.; Zhou, T.; Wu, J.; Li, Y.; Liu, Z.; Xuan, M.; Wua, Y. Euler Force Actuation Mechanism for Siphon Valving in Compact Disk-like Microfluidic Chips. *Biomicrofluidics* **2014**, *8* (2). https://doi.org/10.1063/1.4867241/386103.
(30) Wu, J.; Fang, H.; Zhang, J.; Yan, S. Modular Microfluidics for Life Sciences. *Journal of Nanobiotechnology*. BioMed Central Ltd December 1, 2023. https://doi.org/10.1186/s12951-023-01846-x.
(31) Lai, X.; Yang, M.; Wu, H.; Li, D. Modular Microfluidics: Current Status and Future Prospects. *Micromachines*. MDPI August 1, 2022. https://doi.org/10.3390/mi13081363.
(32) Madou, M.; Lee, L. J.; Daunert, S.; Lai, S.; Shih, C.-H. Design and Fabrication of CD-like Microfuidic Platforms for Diagnostics : Microfuidic Functions. *Biomed Microdevices* **2001**, *3*, 245–254.
(33) Madadelahi, M.; Madou, M. J.; Nokoorani, Y. D.; Shamloo, A.; Martinez-Chapa, S. O. Fluidic Barriers in Droplet-Based Centrifugal Microfluidics: Generation of Multiple Emulsions and Microspheres. *Sens Actuators B Chem* **2020**, *311*, 127833. https://doi.org/10.1016/J.SNB.2020.127833.
(34) Haeberle, S.; Brenner, T.; Schlosser, H. P.; Zengerle, R.; Ducrée, J. Centrifugal Micromixery. *Chem Eng Technol* **2005**, *28* (5), 613–616. https://doi.org/10.1002/CEAT.200407138.
(35) Hessel, V.; Löwe, H.; Schönfeld, F. Micromixers—a Review on Passive and Active Mixing Principles. *Chem Eng Sci* **2005**, *60* (8–9), 2479–2501. https://doi.org/10.1016/J.CES.2004.11.033.
(36) Lee, C. Y.; Wang, W. T.; Liu, C. C.; Fu, L. M. Passive Mixers in Microfluidic Systems: A Review. *Chemical Engineering Journal* **2016**, *288*, 146–160. https://doi.org/10.1016/J.CEJ.2015.10.122.
(37) Soufi, G.; Badillo-Ramírez, I.; Serioli, L.; Altaf Raja, R.; Schmiegelow, K.; Zor, K.; Boisen, A. Solid-Phase Extraction Coupled to Automated Centrifugal Microfluidics SERS: Improving Quantification of Therapeutic Drugs in Human Serum. *Biosens Bioelectron* **2024**, *266*, 116725. https://doi.org/10.1016/J.BIOS.2024.116725.